© 2016. Published by The Company of Biologists Ltd | Journal of Experimental Biology (2016) 219, 1843-1850 doi:10.1242/jeb.138867

RESEARCH ARTICLE

The extraordinary joint material of an articulated coralline alga. II. Modeling the structural basis of its mechanical properties

Mark W. Denny* and Felicia A. King

ABSTRACT

By incorporating joints into their otherwise rigid fronds, erect coralline algae have evolved to be as flexible as other seaweeds, which allows them to thrive – and even dominate space – on wave-washed shores around the globe. However, to provide the required flexibility, the joint tissue of *Calliarthron cheilosporioides*, a representative articulated coralline alga, relies on an extraordinary tissue that is stronger, more extensible and more fatigue resistant than that of other algae. Here, we used the results from recent experiments to parameterize a conceptual model that links the microscale architecture of cell walls to the adaptive mechanical properties of joint tissue. Our analysis suggests that the theory of discontinuous fiber-wound composite materials (with cellulose fibrils as the fibers and galactan gel as the matrix) can explain key aspects of the material's mechanics. In particular, its adaptive viscoelastic behavior can be characterized by two, widely separated time constants. We speculate that the short time constant (~14 s) results from the viscous response of the matrix to the change in cell-wall shape as a joint is stretched, a response that allows the material both to remain flexible and to dissipate energy as a frond is lashed by waves. We propose that the long time constant (~35 h), is governed by the shearing of the matrix between cellulose fibrils. The resulting high apparent viscosity ensures that joints avoid accumulating lethal deformation in the course of a frond's lifetime. Our synthesis of experimental measurements allows us to draw a chain of mechanistic inference from molecules to cell walls to fronds and community ecology.

KEY WORDS: *Calliarthron cheilosporioides*, Genicula, Cell walls, Viscoelasticity, Fiber-reinforced composites, Cellulose fibrils, Galactan matrix, Ecological mechanics

INTRODUCTION

The seaweeds of wave-swept rocky shores survive, in large part, by being flexible, which provides them with the ability to bend and reconfigure when subjected to flow, thereby reducing the imposed hydrodynamic force (Koehl, 1984, 1986; Denny and Gaylord, 2002; Harder et al., 2004; Boller and Carrington, 2006; Martone et al., 2012). The need for flexibility would seemingly pose a problem for coralline red algae, which calcify their cell walls and are therefore inherently rigid. However, some coralline algae – the erect, articulated corallines – have avoided this limitation through the evolution of joints (genicula) that allow their fronds to be as flexible as those of other seaweeds. The flexibility provided by these joints depends on the unusual mechanical properties of the genicular tissue (Martone and Denny, 2008; Janot and Martone, 2016), and these properties are best understood for *Calliarthron cheilosporioides* Manza, a representative articulated coralline found on the West Coast of North America.

Calliarthron cheilosporioides' genicular tissue is 3–5 times more extensible and approximately 4 times stronger than typical algal tissue (B. Hale, Macroalgal materials: foiling fracture and fatigue from fluid forces, PhD thesis, Stanford University, 2001; Martone, 2007; Janot and Martone, 2016), and it is effectively immune to failure by fatigue (Denny et al., 2013). Furthermore, the tissue exhibits an unusual combination of elastic and viscous properties (Denny and King, 2016). As one would expect from an elastic solid, the stress (force per cross-sectional area) required to extend the material increases in proportion to strain (the change in length per unstressed length) (Fig. 1A), and, as is common in many biological solids, the tissue becomes less compliant (i.e. stiffer) the farther it is stretched (Fig. 1B). Neither breaking stress nor the material's compliance (strain per stress) is significantly correlated with the rate of strain, again typical of an elastic solid (Denny and King, 2016). By contrast, other aspects of the tissue's mechanical behavior reveal viscous tendencies. In particular, when subjected to repeated or continuous loads, genicular material accumulates deformation through time with no hint of a plateau (Fig. 2), a behavior characteristic of viscous fluids. In other loading regimes, the interplay of viscous and elastic properties is evident. When cyclically stretched, stress increases with strain during loading as expected of an elastic solid (Fig. 3A, red line), but the unloading curve (black line) falls below the loading curve, an indication that energy is dissipated to heat by viscous processes. An average of 42% of the strain energy required to extend a joint in tension is lost upon retraction, and at least part of this hysteresis can be attributed to unrecovered (that is, plastic) strain, which averages 13% of the maximum strain (arrow in Fig. 3A). Similarly, when a stress cycle is interrupted during extension, stress decreases through time (stress relaxation), a viscous process (Fig. 3B), but, when a cycle is interrupted during retraction, stress in the sample subsequently increases through time (stress recovery), the result of elastic recoil.

Together, these material properties allow genicula to provide the flexibility *C. cheilosporioides*' fronds need to survive – and even dominate space – in the surf zone, while resisting fracture from fatigue and lethal strain from creep (Denny and King, 2016). Indeed, *C. cheilosporioides* can act as an ecosystem engineer: its densely packed fronds serve as a shelter for invertebrate animals.

The unusual mechanical properties of *C. cheilosporioides* genicula stem from the chemical composition and morphology of the cells from which they are constructed, in particular from the chemical composition and morphology of genicular cell walls. We know some basic facts about these cell walls: they form 34% of the cross-sectional area in immature genicula and 54% of the area of mature cells (Martone, 2007), and they are composed of randomly

Hopkins Marine Station of Stanford University, Pacific Grove, CA 93950, USA.

*Author for correspondence (mwdenny@stanford.edu)

M.W.D., 0000-0003-0277-9022

Received 10 February 2016; Accepted 29 March 2016

Journal of Experimental Biology (2016) 219, 1843-1850 doi:10.1242/jeb.138867

List of symbols and abbreviations

c	constant of integration (s)
C	concentration of the matrix gel (mass per mass)
d	diameter of a cellulose fibril (m)
D	tensile compliance (Pa^{-1})
E	tensile modulus (Pa)
E_f	tensile modulus of fibers (Pa)
E_m	tensile modulus of the matrix (Pa)
G_m	shear modulus of the matrix, approximately $E_m/3$ (Pa)
k	orientation coefficient (dimensionless)
L_f	length of a cellulose fibril (m)
t	time (s)
T	time constant (s)
V_f	volume fraction of fibers (dimensionless)
x	variable used in the calculation of η_{max}
ε	strain (dimensionless)
ε_{tot}	total strain of the conceptual model (dimensionless)
η_{max}	efficiency of force transfer from matrix to fibers (dimensionless)
μ	viscosity (Pa s)
σ	stress (Pa)

oriented cellulose fibers in a matrix gel of highly methylated, highly sulfated galactan (Tsekos et al., 1993; Martone et al., 2010; P. T. Martone, unpublished data). However, it is currently unclear how the micro-scale architecture of *C. cheilosporioides*' cell walls is tied to the tissue-scale mechanical properties of this extraordinary material, and thereby to the performance of the fronds in nature.

MATERIALS AND METHODS

To synthesize information from studies characterizing *C. cheilosporioides*' extensibility, compliance, strength, hysteresis and creep – and thereby to understand the mechanisms underlying the alga's ecological interactions – we propose a conceptual model of genicular cell wall material in which elastic elements (springs of a given stiffness) and viscous elements (dashpots of a given viscosity) are combined in the simplest possible configuration capable of mimicking the behavior of genicular material (Fig. 4).

The model is based on the idealized properties of springs and dashpots. For an ideal spring, stress (σ) is linearly proportional to strain (ε), with modulus E as the constant of proportionality:

$$\sigma = E\varepsilon. \quad (1)$$

By contrast, for an ideal dashpot, stress is linearly proportional to strain rate, with viscosity μ as the constant of proportionality:

$$\sigma = \mu\frac{d\varepsilon}{dt}. \quad (2)$$

Stress has units of newtons per square meter (i.e. pascals), viscosity has units of pascal-seconds and strain is dimensionless.

In our model, spring 1 and dashpot 1 are connected in parallel, forming a Voigt element whose overall stiffness depends on strain rate (Aklonis et al., 1972). At low strain rate, the viscosity of the dashpot, μ_1, makes a negligible contribution to stiffness, and the Voigt element's overall stiffness is approximately E_1, that of spring 1 alone. At sufficiently high strain rates, the spring's stiffness is negligible compared with that of the dashpot, and the Voigt element's overall stiffness is thus that of dashpot 1 alone. At intermediate strain rates, both the spring and dashpot contribute to stiffness. Note that a Voigt element can creep only until the load borne by the spring is equal to the applied stress. The time required

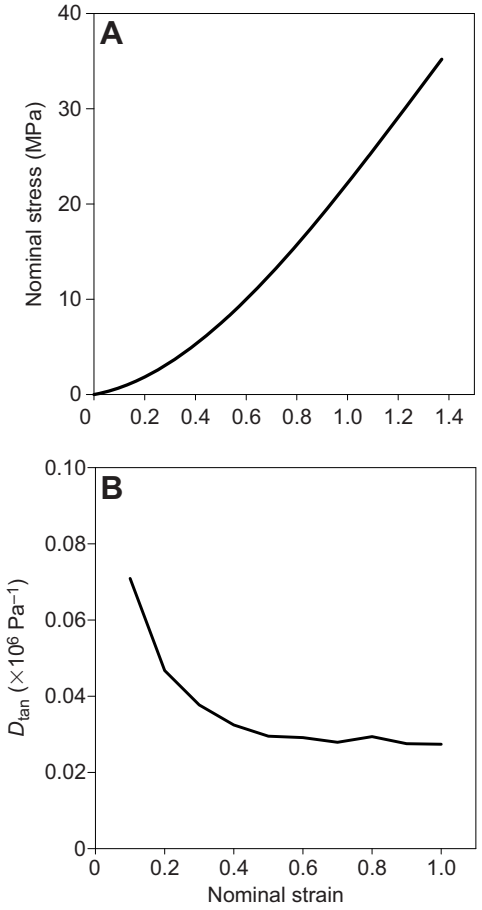

Fig. 1. The behavior of genicular material in high strain rate tensile tests. D_{tan}, tangential compliance. Modified from fig. 6A,B in Denny and King (2016).

to approach this equilibrium (the element's time constant, T_1) is (Aklonis et al., 1972):

$$T_1 = \frac{\mu_1}{\sigma}. \quad (3)$$

Spring 2 and dashpot 2 are connected in series, forming a Maxwell element, whose behavior is the converse of that of the Voigt element. At low strain rates, dashpot 2 offers little resistance. As a result, spring 2 is not stretched, and the element's overall stiffness is therefore governed by the viscosity of dashpot 2, μ_2. At high strain rates, dashpot 2 is essentially frozen and the element's stiffness is that of spring 2, E_2. Unlike the Voigt element, the Maxwell element creeps without limit when a constant stress is imposed. The response time for the Maxwell element is (Aklonis et al., 1972):

$$T_2 = \frac{\mu_2}{\sigma}. \quad (4)$$

These relationships allow us to estimate E_2 and μ_2 in our model using data from experiments regarding stiffness and creep reported in the companion paper (Denny and King, 2016). When the entire model is strained at a sufficiently high rate, both dashpots are 'frozen' and the model's stiffness is due to spring 2 alone. Thus, E_2 is approximately equal to the modulus measured for genicula at very high strain rates. If a constant stress is applied instead of a constant strain rate, the model experiences an instantaneous strain as spring 2 stretches. Additional strain then accrues as both dashpots relax. Eventually, spring 1 comes into equilibrium with the applied stress,

Journal of Experimental Biology (2016) 219, 1843-1850 doi:10.1242/jeb.138867

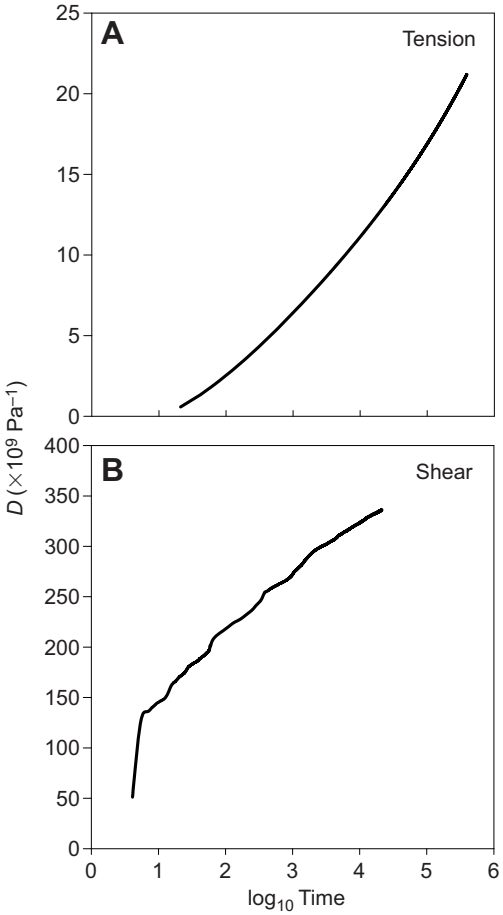

Fig. 2. Average creep behavior of genicular material. (A) Creep in tension. (B) Creep in shear. *D*, compliance. Time was measured in s. A and B are reproduced from the companion paper (Denny and King, 2016) for ease of reference.

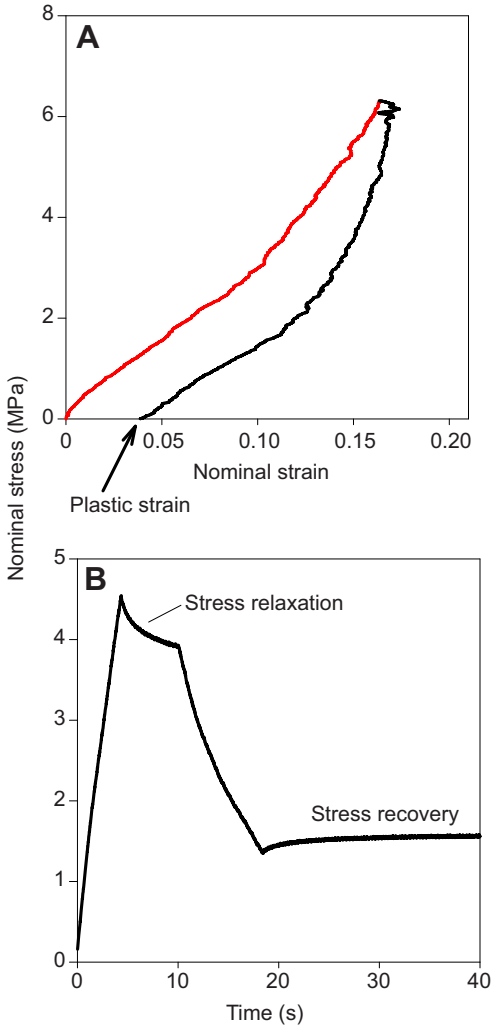

Fig. 3. Results from the cyclic tensile tests. (A) Representative results from the initial cycle of strain. (B) A test showing stress relaxation when extension is stopped while stress is increasing, and stress recovery when retraction is subsequently stopped as stress decreases. A and B are, respectively, modified and reproduced from the companion paper (Denny and King, 2016).

and the Voigt element ceases to extend. But overall strain accrues as dashpot 2 continues to extend, and for times much greater than T_1, the increase in strain is due solely to the extension of dashpot 2. Thus:

$$\mu_2 \approx \frac{\sigma}{d\varepsilon/dt}, \quad (5)$$

where $d\varepsilon/dt$ is the strain rate measured in a tensile creep test well after the imposition of stress. Through a series of mathematical manipulations (see Appendix 1), we can use our experimental data to estimate μ_1:

$$\mu_1 = -\frac{E_2^2 \varepsilon_{tot}}{d\sigma/dt}, \quad (6)$$

where $d\sigma/dt$ is evaluated at the initiation of a stress relaxation experiment (described below). This leaves E_1 as a free parameter that we can estimate by choosing the value that allows the model to best match experimental results. Once values have been established for E_1, E_2, μ_1 and μ_2, we can calculate how the model will behave for any time course of applied stress or strain (see Appendix 2).

In summary, we can use experimental data to populate a mathematical model of genicular material properties, by extension providing a means to tie cell wall structure to frond-scale performance.

RESULTS

From the high strain rate experiments conducted in the companion paper (Denny and King, 2016), we estimate that E_2 (at ε=0.2, a strain typical of our cyclical stress–strain experiments) is approximately 27 MPa. From the average creep of genicula in tension (Denny and King, 2016), we estimate (using Eqn 5) that μ_2 is approximately 5×10^{12} Pa s, and from stress relaxation tests (Denny and King, 2016), we estimate that μ_1 is approximately 3.9×10^{8} Pa s. Through trial and error, we then estimate that E_1 is 40 MPa. The response times T_1 and T_2 are thus 14 s and 35 h, respectively (Eqns 3 and 4).

Using these values, the model mimics (qualitatively and, roughly, quantitatively) much of the tensile behavior of genicula as measured in our experiments (Fig. 5). A cycle to a stress of 3.63 MPa at a strain rate of 0.017 s^{-1} has a hysteresis of 35.5% with a plastic strain of 0.038, 22% of maximum strain (Fig. 5A, compare with Fig. 3A). (The stiffness of the model is slightly lower than that of the specimen shown in Fig. 3A, but this is expected because this particular specimen's stiffness was above average.) The model exhibits stress relaxation after an increase in stress and stress

Journal of Experimental Biology (2016) 219, 1843-1850 doi:10.1242/jeb.138867

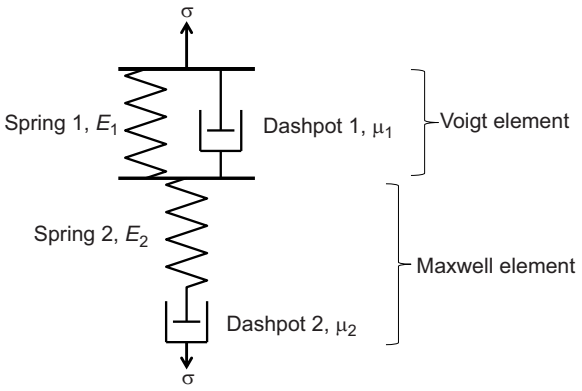

Fig. 4. The conceptual spring-and-dashpot model of genicular material. σ, stress; μ, viscosity; *E*, elastic modulus.

recovery after a decrease in stress (Fig. 5B, compare with Fig. 3B). The model's modulus increases with increasing strain rate, but only for rates less than approximately 0.1 s^{-1} (Fig. 5C); at the higher strain rates used in actual measurements (0.2–825), the model's compliance is independent of strain rate, as it was in the experiments. The model overestimates the creep compliance of genicular material by a factor of 4–7 (for reasons we address in the Discussion), but qualitatively reproduces the material's behavior: at long times (>1000 s), the model continues to creep in tension without a hint of a plateau, as it does in the real material (Fig. 5D, compare with Fig. 2A). For times less than approximately 20 s, the model creeps rapidly, as genicular material did for our (Denny and King, 2016) experiments in shear (Fig. 5D, compare with Fig. 3B). Note that, because the model predicts compliance in tension rather than shear, this last comparison can be made only qualitatively.

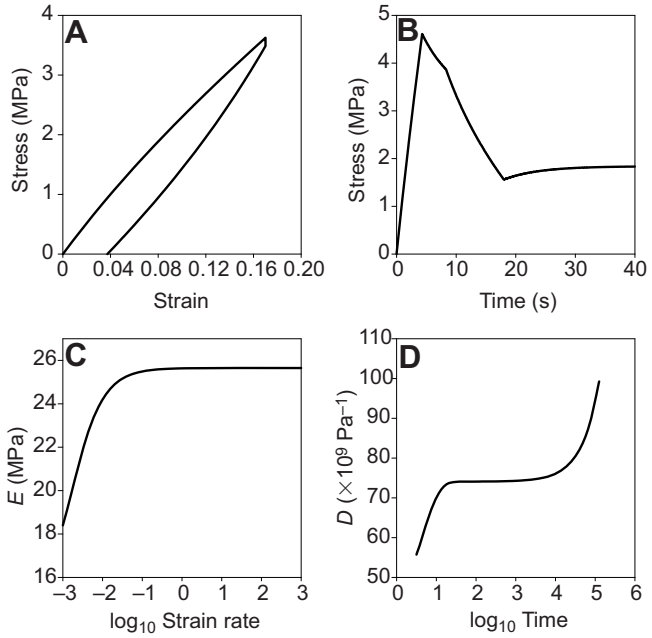

Fig. 5. The behavior of the conceptual model. (A) A stress–strain cycle. (B) Stress relaxation and stress recovery. (C) Elastic modulus (*E*) as a function of strain rate (measured as s^{-1}). (D) Compliance (*D*) as a function of time (creep; measured in s).

DISCUSSION

The ability of our model to mimic the behavior of genicular material is due to the interplay between its characteristic elastic moduli (E_1 and E_2) and its characteristic viscosities (μ_1 and μ_2). E_1 and E_2 are so similar (27 and 40 MPa) that we can think of them as a single characteristic stiffness, E. But μ_1 and μ_2 are vastly different (μ_1=3.9×10^8 Pa s, μ_2=5×10^{12} Pa s), which has two important consequences. On the one hand, a Voigt element's viscous nature is apparent only for stresses that are applied for periods comparable to T_1 (=μ_1/E). For loads applied more rapidly, the whole element is essentially frozen; for loads applied for longer periods, only E matters. Because μ_1 is relatively low, T_1 is of the order of 10 s, which explains genicular material's hysteresis and plastic deformation in short-term cyclic tests, its short-term stress relaxation and stress recovery behavior, and the initial rapid creep seen in the shear tests. On the other hand, dashpot 2's viscosity is so high (13,000 times that of μ_1) that the time constant for the Maxwell element (=μ_2/E) is of the order of 1.5 days. As a consequence, the Maxwell element's viscous nature is evident only for loads applied over many hours, accounting for the fact that genicular material can creep in the long term, yet avoid accruing lethal strain during a frond's lifetime. In short, our heuristic model suggests that the mechanical behavior of genicular cell walls is due to a single elastic structural element, and structural elements that involve two different viscous responses.

These results allow us to form a tentative understanding of the mechanics that link cell wall chemistry and structure to material properties, and thereby to the alga's function in nature. We suggest that the springs and dashpots of our model correspond (at least roughly) to the structural attributes of genicular micro-architecture – to the cellulose fibrils and galactan matrix, respectively. We propose that both E_1 and E_2 are provided by discontinuous cellulose fibrils. If these fibrils are long compared with their diameter (as is typical of cellulose), shear between fibrils and the matrix can effectively transfer stress to the fibrils, allowing them to act as the primary bearers of an imposed tensile load (Bunsell and Renard, 2005; Gosline, 2017). The slight difference between our estimates of E_1 and E_2 (27 MPa versus 40 MPa) may or may not be significant. Perhaps the stiffness of fibrils differs between the primary and secondary cell walls, accounting for the difference in moduli. However, it seems equally likely that the apparent difference between E_1 and E_2 is an artifact of our tweaking the model; the model is only marginally less realistic if E_2=E_1=27 MPa. Note that the model tacitly assumes that fibrils are discontinuous; if they were continuous from one end of a cell to the other, the material could not creep without limit as it apparently does.

While it is reasonably clear that cellulose fibrils act as springs, the correspondence of cell wall architecture to the model's dashpots is more nuanced. In the model, overall tensile compliance is accounted for by two dashpots that differ drastically in their viscosity. Thus, because stress is equal to the product of viscosity and strain rate (Eqn 2), when a given strain rate is applied to the model, the different viscosities produce different stresses. However, we can instead suppose that, in the cell wall, there is only one viscosity – that of the galactan gel – but that two strain rates act as the material is deformed. From this perspective, the apparent difference in dashpot viscosity (μ_1=3.9×10^8 Pa s and μ_2=5×10^{12} Pa s) is due to variation in how the matrix is strained locally. We propose that μ_1 is the viscous reaction of the matrix to bulk shear as a cell extends. Even in the absence of any interaction with cellulose fibrils, the matrix is sheared during extension as the cell wall changes shape – lengthening axially and contracting laterally; μ_1 is the viscous reaction to the rate of this shear. By contrast, we propose that μ_2 is

Journal of Experimental Biology (2016) 219, 1843-1850 doi:10.1242/jeb.138867

due to the viscous reaction of the material as the discontinuous cellulose fibrils slide past each other, shearing the matrix between them. For a given overall tensile strain rate, local shear strain rate in the matrix confined between sliding fibrils is likely to be much greater than the bulk shear accounting for μ_1, resulting in our calculation of a relatively large value of μ_2. Any direct viscous interaction between cellulose fibrils (e.g. the slippage of entangled fibrils) would also contribute to μ_2.

As a tentative test of our mechanistic, structural perspective on the material properties of genicular material, we can use the theory of fiber-reinforced composites to predict the material's tensile elastic compliance. As suggested above, we assume that cellulose fibrils act as the discontinuous, randomly oriented fibers in the composite and galactan gel acts as the matrix. Simple theory (Bunsell and Renard, 2005; Gosline, 2016) suggests that:

$$D = \frac{1}{E} = \frac{1}{k\,\eta_{max} V_f E_f + (1 - V_f) E_m}, \quad (7)$$

where D is the material's overall tensile compliance, E is the material's overall tensile modulus, E_f is the tensile modulus of the fiber, E_m is the tensile modulus of the matrix and V_f is the fraction of the material's volume occupied by fibers. Coefficient k accounts for the orientation of fibers relative to the direction of applied force; k is 1 for fibers in line with force and 0 for fibers perpendicular to force. When fibers are randomly oriented, as they are in *C. cheilosporioides*' cell walls, k=0.375.

Gosline (2016) provides equations for estimating η_{max}, the maximum efficiency with which stress can be transferred from matrix to fibers. First, one calculates x:

$$x = \frac{L_f}{d}\sqrt{\frac{2G_m}{E_f \ln\left(\frac{1}{\sqrt{V_f}}\right)}}, \quad (8)$$

where L_f and d are the length and diameter of the fibers, respectively, and G_m is the shear modulus of the matrix material (approximately one third E_m). Transfer efficiency is then:

$$\eta_{max} = 1 - \frac{\tanh(x)}{x}. \quad (9)$$

Martone (P. T. Martone, Biomechanics of flexible joints in the calcified seaweed *Calliarthron cheilosporioides*, PhD thesis, Stanford University, 2007) found that cellulose and galactans formed equal fractions (15%) of the dry mass of genicula. If we assume that cellulose and galactans are the dominant structural components of the cell wall, and that the swelling in water of galactans as they form a gel is much greater that of cellulose fibrils, we can estimate V_f (Appendix 3):

$$V_f \approx \frac{1}{1 + (1/C)}, \quad (10)$$

where C is the concentration of galactan in the hydrated matrix gel. For example, if the matrix is a 1% gel, the volume of gel is approximately 100 times that of dry galactan, and therefore 100 times that of cellulose; V_f is thus 0.0099. Wainwright et al. (1976) suggest that the modulus of wet cellulose in terrestrial plant cell walls is approximately 3×10^{10} Pa, and we can guess that the tensile modulus of galactan gel is similar to that of agar (a cell wall component of some other red algae), which ranges from 0.023 MPa at 0.5% concentration to 0.53 MPa at 5% concentration (Nayar et al., 2012). Inserting these values into Eqns 7–10 gives the results shown in Fig. 6. At a gel concentration of 1%, the observed compliance of genicular material (3.7×10^{-8} Pa^{-1}) is obtained if cellulose fibers have an aspect ratio of approximately 1200. The higher the galactan concentration, the shorter the fibers need to be to result in the observed compliance. At a 5% concentration, fibrils need have an aspect ratio of only ~200. Gosline (2017) suggests that the aspect ratio of cellulose fibrils in terrestrial plants is at least 1000, so the aspect ratios required to match the observed compliance seem feasible. In summary, it seems likely that the measured tensile stiffness of genicula can be explained by treating the material as a two-part composite comprising cellulose fibrils and galactan matrix.

Note that Fig. 6 implies that genicula should become less compliant as they desiccate: the aspect ratio of fibrils stays the same, but the concentration of the gel increases as water is lost. Casual observation reveals that genicula do indeed become leathery and then stiffly brittle as they dry out.

Although this theoretical analysis (Eqn 7) is consistent with our proposed explanation of cell wall mechanics, it is important to note that it addresses only the static elastic nature of the material. Our conceptual model suggests that, at very low strain rates, the compliance of the material ($1/\varepsilon$) is strain-rate dependent (Fig. 5C). Thus, the compliance predicted by Eqn 7 in fact depends on how E_m varies with strain rate, and that information is not currently available. Further verification of our explanation of cell wall mechanics awaits more detailed examination of the properties of the matrix gel and its interaction with cellulose fibrils.

Our approach to the mechanics of *C. cheilosporioides*' genicula can potentially be applied to the joints of other articulated coralline algae. However, the morphology, chemistry and mechanical properties of joints vary substantially among taxa (e.g. Johansen, 1981; Janot and Martone, 2016). To determine whether our approach has general utility, we must wait until the necessary measurements (chemical content, ultrastructure, cyclic and high strain rate stress–strain characteristics, creep) have been made for a representative sampling of species.

Caveats

There are several aspects of our conceptual model that must be taken with a grain of salt. For example, the model predicts that, across the

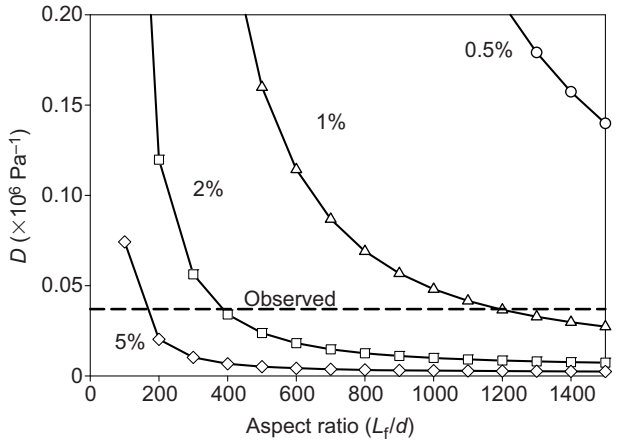

Fig. 6. The results of the fiber-reinforced composite model of cell wall tensile modulus. The higher the aspect ratio of cellulose fibrils, the lower the concentration of galactan gel required to produce the observed tensile modulus. D, compliance; L_f, length of a cellulose fibril; d, diameter of a cellulose fibril.

Journal of Experimental Biology (2016) 219, 1843-1850 doi:10.1242/jeb.138867

range of strain rates used in our tests, tensile compliance is independent of strain and equal to $1/E_2$. In reality, D_{tan} decreases with increasing strain (Fig. 1B), likely because cellulose fibrils reorient. (In fiber-reinforced composite theory, this would be accounted for by an increasing k.) A more accurate spring-and-dashpot model would need to specify that spring 2 has non-linear characteristics in which E_2 increases with increasing strain.

Our model overestimates the compliance measured for actual genicula. This discrepancy may be due in part to the fact that our estimates of E_1, E_2 and μ_1 are based on experiments conducted at 19–20°C, while the tensile creep experiments (from which μ_2 was estimated) were conducted at 12–13°C (Denny and King, 2016). In general, the compliance of viscoelastic materials is lower at lower temperatures (Ferry, 1980; Gosline, 2017). Until the tensile creep tests are repeated at higher temperatures, we will not know how much of the discrepancy can be explained by temperature alone.

Another limitation of the model is revealed when we use it to predict the behavior of genicular material in a dynamic test in which a geniculum is strained sinusoidally at a range of frequencies. In this experiment, there are two relevant metrics. The storage modulus, E', is the portion of the overall stiffness of the material that is due to elasticity and is therefore in phase with the sinusoidally varying strain. By contrast, the loss modulus, E'', is the portion of the overall stiffness that is due to viscosity. Because the stiffness of a viscous material is proportional to the rate of strain, E'' is the portion of the overall stiffness that is 90 deg out of phase with the driving strain (Aklonis et al., 1972; Wainwright et al., 1976; Ferry, 1980). The model predicts the behavior shown by the solid red lines in Fig. 7: E' increases with increasing frequency of loading, but only at the low frequencies corresponding to the Voigt element's time constant ($f=1/T_1=0.07$ Hz). At higher frequencies, E' is virtually constant and approximately equal to E_2. Our model predicts that E'' is substantial only for a small range of frequencies around 0.07 Hz. These predictions are only a rough match to actual dynamic measurements on *C. cheilosporioides*' genicula (Denny and Gaylord, 2002), shown by the dashed black lines in Fig. 7. In those experiments, E' increased gradually with frequency, while E'' was nearly constant across the entire range of frequencies.

These comparisons (creep compliance, dynamic stiffness) suggest that our heuristic model is too simple to be entirely accurate. Rather than a single dashpot in each of the Voigt and Maxwell elements, a more accurate model would employ a spectrum of dashpots with a range of viscosities. Such a spectrum could capture cell wall architecture and mechanics in greater detail. For example, at a given overall strain rate, local strain rate (and thereby apparent viscosity) may well vary with the local angle between cellulose fibrils and the applied force; the random arrangement of cellulose fibrils would result in a range of effective viscosities for both μ_1 and μ_2. A model incorporating a spectrum of dashpots could more closely mimic the dynamic properties of genicular tissue. Such a spectrum of dashpots could also produce a model whose creep characteristics are more similar to Fig. 2A than are those of our current model (Fig. 5D). However, it was not our intent to model genicular material as accurately as possible; rather, our intention was to model the material as simply as possible, and thereby gain insight into the connection between microscale structure and material properties. The model we propose here, rough as it is, suits this purpose.

We note again that our model provides predictions for genicular material only in tension. The behavior of genicula in shear is governed in large part by the properties of the middle lamina. Other than showing that compliance in shear is greater than that in tension, our tests have no ability to inform us about the properties of the middle lamina.

Lastly, in our companion paper (Denny and King, 2016), we report that, while breaking stress of genicular material is independent of strain rate, breaking strain increases with increasing strain rate. Our model offers no insight into this unusual behavior. The faster the material is stretched, the less time cellulose fibrils have to slip past each other before breaking stress is reached, so one might suppose that, in as much as breaking strain is proportional to how far fibrils slide, breaking strain would decrease with increasing strain rate. However, it is possible that tensile failure is initiated not by the average strain of the material, but rather by local strains. If, in the course of a slow stretch, the material is locally weakened as a few errant fibers have time to slide relative to each other, that local flaw could potentially trigger failure at relatively low overall strain. The faster the material is strained, the more resistant fibrils are to sliding past each other, making it less likely that local effects can proceed to the point where they trigger failure. The overall strain at breakage could thereby increase with increasing strain rate. However, this explanation is pure speculation.

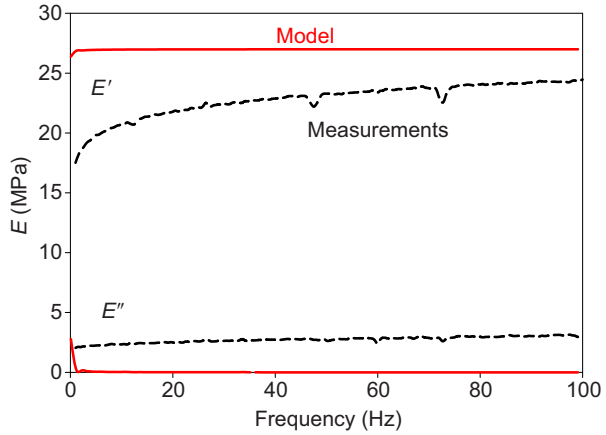

Fig. 7. A comparison of model results (solid red lines) and empirical measurements (dashed black lines) of storage and loss moduli. E', storage modulus; E'', loss modulus. Drawn using data from Denny and Gaylord (2002).

Conclusions

The joint material of *C. cheilosporioides* is viscoelastic. On the one hand, its compliance is independent of strain rate across a wide range of strain rates – characteristic of an elastic solid – which allows joints to maintain their flexibility when loaded by the rapidly imposed hydrodynamic forces of breaking waves. On the other hand, because cellulose fibrils in cell walls are discontinuous, genicular material can creep – a characteristic of a viscous fluid. Viscosity causes the joints to dissipate much of the strain energy absorbed during cyclic wave loading – potentially reducing the chance of fatigue failure – and the viscosity of the cell wall matrix is sufficient so that creep may increase joint flexibility while preventing joints from gradually stretching to the point of failure. We tentatively assign structural elements of the cell wall to the elastic and viscous elements of a conceptual, spring-and-dashpot model that successfully mimics genicular performance, thereby allowing us to connect mechanism across scales, from the molecular architecture of cell walls to the properties of genicular tissue to the function of entire fronds in their ecological context.

Journal of Experimental Biology

Journal of Experimental Biology (2016) 219, 1843-1850 doi:10.1242/jeb.138867

Appendix 1

Our objective here is to formulate an expression for the manner in which applied stress is related to the strain of our spring-and-dashpot model. By referring to Fig. 4, we see that the overall strain of the model, ε_{tot}, is the sum of the strains of the Voigt and Maxwell elements. At the initiation of extension, the dashpot in the Maxwell element does not have time to extend, so the initial strain in the element is that of spring 2 alone. Furthermore, because the Voigt element and spring 2 are in series, they experience the same stress. Thus, using Eqns 1 and 2, we set the initial stress of spring 2 (the product of the spring's modulus and strain) equal to the stress of the Voigt element:

$$\sigma = E_2(\varepsilon_{tot} - \varepsilon_1) = E_1\varepsilon_1 + \mu_1\frac{d\varepsilon_1}{dt}. \quad (A1)$$

Solving for $d\varepsilon_1/dt$:

$$\frac{d\varepsilon_1}{dt} = \frac{E_2\varepsilon_{tot}}{\mu_1} - \frac{(E_1+E_2)\varepsilon_1}{\mu_1}. \quad (A2)$$

To simplify mathematical manipulation, let:

$$x = \frac{E_2\varepsilon_{tot}}{\mu_1}, \quad (A3)$$

$$y = -\frac{E_1+E_2}{\mu_1}. \quad (A4)$$

Thus:

$$\frac{d\varepsilon_1}{dt} = x + y\varepsilon_1. \quad (A5)$$

We then proceed to solve this differential equation:

$$\int dt = \int \frac{1}{x+y\varepsilon_1}d\varepsilon_1, \quad (A6)$$

$$t = \frac{\ln(x+y\varepsilon_1)}{y} + c, \quad (A7)$$

where c is the constant of integration. Rearranging:

$$yt = \ln(x+y\varepsilon_1) + yc. \quad (A8)$$

At t=0, ε_1=0, so:

$$c = -\frac{\ln(x)}{y}. \quad (A9)$$

Substituting this value for c into Eqn A8 and rearranging:

$$yt + \ln(x) = \ln(x+y\varepsilon_1), \quad (A10)$$

$$\exp[yt + \ln(x)] = x + y\varepsilon_1, \quad (A11)$$

$$\varepsilon_1 = \frac{1}{y}\exp[yt + \ln(x)] - \frac{x}{y}. \quad (A12)$$

With this expression for ε_1 in hand, we can return to the first part of Eqn A1:

$$\sigma = E_2(\varepsilon_{tot} - \varepsilon_1), \quad (A13)$$

$$\sigma = E_2\varepsilon_{tot} - \frac{E_2}{y}\exp[yt + \ln(x)] + \frac{E_2x}{y}. \quad (A14)$$

Substituting the full expressions for x and y, we arrive at an expression describing how our model would behave in a stress relaxation test in which stress is measured through time subsequent to the imposition of an initial strain, ε_{tot}:

$$\sigma = E_2\varepsilon_{tot} + \frac{E_2\mu_1}{E_1+E_2}\exp\left[-\left(\frac{E_1+E_2}{\mu_1}\right)t + \ln\left(\frac{E_2\varepsilon_{tot}}{\mu_1}\right)\right] - \frac{E_2^2\varepsilon_{tot}}{E_1+E_2}. \quad (A15)$$

We then use this expression to provide a recipe for estimating μ_1. Taking the temporal derivative of Eqn A15:

$$\frac{d\sigma}{dt} = -E_2\exp\left[-\left(\frac{E_1+E_2}{\mu_1}\right)t + \ln\left(\frac{E_2\varepsilon_{tot}}{\mu_1}\right)\right]. \quad (A16)$$

The initial slope ($d\sigma/dt$) of a stress relaxation experiment in which strain is applied abruptly (that is, ε=ε_{tot} at t=0) is thus:

$$\frac{d\sigma}{dt} = -E_2\exp\left[\ln\left(\frac{E_2\varepsilon_{tot}}{\mu_1}\right)\right] = -\frac{E_2^2\varepsilon_{tot}}{\mu_1}. \quad (A17)$$

We can now solve for μ_1:

$$\mu_1 = -\frac{E_2^2\varepsilon_{tot}}{d\sigma/dt}, \quad (A18)$$

where $d\sigma/dt$ is evaluated at the initiation of stress relaxation.

Appendix 2

The behavior of our model in response to a given time course of strain was solved numerically. The following pseudocode illustrates the algorithm. Here, $\Delta\varepsilon_{tot}(t)$ is the change in overall strain imposed in a particular increment in time, Δt; $\Delta\varepsilon_{tot}(t)$ can be positive for extension, or negative for retraction, of the apparatus imposing the strain. The magnitude and sign of $\Delta\varepsilon_{tot}(t)$ is specified by the type of experiment being conducted.

Initial conditions:

ε_{tot}=ε_1=ε_2=ε_3=σ=0.

Here, ε_1 is the strain of the Voigt element, ε_2 is the strain of spring 2 and ε_3 is the strain of dashpot 2.

For time t=Δt to the end of the experiment in increments Δt:

$\varepsilon_{tot}(t)$=$\varepsilon_{tot}(t-\Delta t)$+$\Delta\varepsilon_{tot}(t)$: increment the overall strain

$\varepsilon_2(t)$=$\varepsilon_{tot}(t)$−$\varepsilon_1(t-\Delta t)$−$\varepsilon_3(t-\Delta t)$: calculate the strain in spring 2

$\sigma(t)$=E_2×$\varepsilon_2(t)$: spring 2 acts as a force transducer allowing us to calculate stress

$\Delta\varepsilon_3$=Δt×[$\sigma(t)$ / μ_3]: calculate the increment in strain in dashpot 2

$\varepsilon_3(t)$=$\varepsilon_3(t-\Delta t)$+$\Delta\varepsilon_3$: calculate the new strain in dashpot 2

$\Delta\varepsilon_1$=Δt×{$\sigma(t)$−[E_1×$\varepsilon_1(t-\Delta t)$]}/$\mu_1$: calculate the increment in Voigt element strain

$\varepsilon_1(t)$=$\varepsilon_1(t-\Delta t)$+$\Delta\varepsilon_1$: calculate the new strain in the Voigt element

Iterate.

For the calculations to be accurate, the increment in time must be kept short; we used Δt=0.001 s. The efficiency of the numerical solution can be increased by implementing this basic procedure in a 4th order Runge–Kutta algorithm, but there is negligible increase in accuracy for the types of simple experiments documented in this study (linear strain ramps with slow stress relaxation/recovery, dynamic test with small-amplitude sinusoidal strain).

The behavior of the model in creep can be described analytically. Under the influence of a constant stress, σ, the strain of a Maxwell

element is (Aklonis et al., 1972):

$$\varepsilon_{\mathrm{M}}(t) = \frac{\sigma}{E} + \frac{\sigma t}{\mu}, \quad \text{(A19)}$$

For a Voigt element:

$$\varepsilon_{\mathrm{V}}(t) = \frac{\sigma}{E}\left[1 - \exp\left(-\frac{tE}{\mu}\right)\right]. \quad \text{(A20)}$$

Thus, for our model, with Maxwell and Voigt elements connected in series:

$$\varepsilon_{\mathrm{tot}}(t) = E_{\mathrm{M}} + E_{\mathrm{V}} = \frac{\sigma}{E_2} + \frac{\sigma t}{\mu_2} + \frac{\sigma}{E_1}\left[1 - \exp\left(-\frac{tE_1}{\mu_1}\right)\right]. \quad \text{(A21)}$$

Appendix 3

Eqn 10 is based on three assumptions. First, we assume that the entire volume of the cell wall consists only of fibers (with volume fraction V_{f}) and hydrated matrix (with volume fraction V_{m}). That is:

$$V_{\mathrm{f}} + V_{\mathrm{m}} = 1. \quad \text{(A22)}$$

Next, based on measurements, we assume that (for a given volume of cell wall) the mass of cellulose in fibers is equal to the mass of galactan in the gel, which implies that the volume of cellulose is approximately equal to the volume of galactan. Further, assuming that the volumetric concentration of galactan in the gel, CV_{f}, is roughly equal to it mass concentration, the equality of cellulose and galactan masses tells us that:

$$V_{\mathrm{f}} \approx CV_{\mathrm{m}}, \quad \text{(A23)}$$

$$V_{\mathrm{m}} \approx \frac{V_{\mathrm{f}}}{C}. \quad \text{(A24)}$$

Substituting this value for V_{m} into Eqn A23 and solving for V_{f}, we arrive at Eqn A25:

$$V_{\mathrm{f}} = \frac{1}{1 + (1/C)}. \quad \text{(A25)}$$

This approximation is only as accurate as its assumptions, which are unlikely to be precisely met in *C. cheilosporioides*' cell walls. We know, for instance, that there are other cell wall constituents besides cellulose and galactan. But for the present purposes, only a rough approximation is required.

Acknowledgements

We thank Sarah Tepler and Tad Finkler for assistance with the experiments that formed the basis for this synthesis, and Patrick Martone for advice and insight regarding all aspects of *C. cheilosporioides*' mechanics and natural history. This work is dedicated to John Gosline, who taught us how to think about materials.

Competing interests

The authors declare no competing or financial interests.

Author contributions

F.A.K. and M.W.D. collaborated on the conception of the heuristic model. M.W.D. carried out the model simulations, and was primarily responsible for writing the manuscript.

Funding

This work was funded by National Science Foundation grants IOS-0641068 and IOS-1130095 to M.W.D., for which we are grateful.

References

Aklonis, J. J., MacKnight, W. J. and Shen, M. (1972). *Introduction to Polymer Viscoelasticity*. New York: Wiley-Interscience.

Boller, M. L. and Carrington, E. (2006). The hydrodynamic effects of shape and size change during reconfiguration of a flexible macroalga. *J. Exp. Biol.* **209**, 1894-1903.

Bunsell, A. R. and Renard, J. (2005). *Fundamentals of Fibre Reinforced Composite Materials*. Briston, UK: Institute of Physics Publishing.

Denny, M. W. and Gaylord, B. (2002). The mechanics of wave-swept algae. *J. Exp. Biol.* **205**, 1355-1362.

Denny, M. W. and King, F. A. (2016). The extraordinary joint material of an articulated coralline alga. I. Mechanical characterization of a key adaptation. *J. Exp. Biol.* **219**, 1833-1842.

Denny, M., Mach, K., Tepler, S. and Martone, P. (2013). Indefatigable: an erect coralline alga is highly resistant to fatigue. *J. Exp. Biol.* **216**, 3772-3780.

Ferry, J. D. (1980). *Viscoelastic Properties of Polymers*, 3rd edn. New York: John Wiley and Sons.

Gosline, J. M. (2017). *Principles of Structural Biomaterials*. Berkeley, California: University of California Press (in press).

Harder, D. L., Speck, O., Hurd, C. L. and Speck, T. (2004). Reconfiguration as a prerequisite for survival in highly unstable flow-dominated habitats. *J. Plant Growth Regul.* **23**, 98-107.

Janot, K. and Martone, P. T. (2016). Convergence of joint mechanics in independently evolving, articulated coralline algae. *J. Exp. Biol.* **219**, 383-391.

Johansen, H. W. (1981). *Coralline Algae, a First Synthesis*. Boca Raton, Florida: CRC Press.

Koehl, M. A. R. (1984). How do benthic organisms withstand moving water? *Am. Zool.* **24**, 57-70.

Koehl, M. A. R. (1986). Seaweeds in moving water: form and mechanical function. In *On the Economy of Plant Form and Function* (ed. T. J. Givnish), pp. 603-634. Cambridge, UK: Cambridge University Press.

Martone, P. T. (2007). Kelp versus coralline: cellular basis for mechanical strength in the wave-swept seaweed *Calliarthron* (Corallinaceae, Rhodophyta). *J. Phycol.* **43**, 882-891.

Martone, P. T. and Denny, M. W. (2008). To bend a coralline: effect of joint morphology on flexibility and stress amplification in an articulated calcified seaweed. *J. Exp. Biol.* **211**, 3421-3432.

Martone, P. T., Navarro, D., Stortz, C. and Estevez, J. M. (2010). Differences in polysaccharide structure between calcified and uncalcified segments in the coralline *Calliarthron cheilosporioides* (Corallinales, Rhodophyta). *J. Phycol.* **46**, 507-515.

Martone, P. T., Kost, L. and Boller, M. (2012). Drag reduction in wave-swept macroalgae: alternative strategies and new predictions. *Am. J. Bot.* **99**, 806-815.

Nayar, V. T., Weiland, J. D., Nelson, C. S. and Hodges, A. M. (2012). Elastic and viscoelastic characterization of agar. *J. Mech. Behav. Biomed. Materials* **7**, 60-68.

Tsekos, I., Reiss, H.-D. and Schnepf, E. (1993). Cell-wall structure and supramolecular organization of the plasma membrane of marine red algae visualized by freeze-fracture. *Acta Bot. Neerl.* **42**, 119-132.

Wainwright, S. A., Biggs, W. D. Currey, J. D. and Gosline, J. M. (1976). *Mechanical Design in Organisms*. Princeton, New Jersey: Princeton University Press.

Journal of Experimental Biology